$LaBr_3(Ce)$: a new generation detector for timing spectroscopy

Sourav Kumar Dey

Saha Institute of Nuclear Physics

February 15, 2017

Contents

- Properties of common inorganic scintillators
- Characterization of $LaBr_3$(Ce) and BaF_2 detectors
- Application of $LaBr_3$(Ce) and BaF_2 scintillators in perturbed angular correlation (PAC) spectroscopy
  - Principle
  - Experimental details
  - Studies in $HfNi_3$ alloy
- Conclusion

Application of scintillation detectors

- Nuclear energy and timing spectroscopy (TDPAC, Positron annihilation spectroscopy)
- High energy physics experiments
- Dark matter search experiment (to detect the recoil spectrum by WIMS)
- Geological exploration
- Medical imaging (PET)

Characteristics of an ideal scintillator

- High Z and density (for high detection efficiency)
- High light output and linearity with energy (for energy spectroscopy)
- Fast response time (for timing spectroscopy)
- Transparent to emitted light (for minimum loss of light)
- Non hygroscopic
- Low afterglow

Properties of common inorganic scintillator

Scintillators	Light yield (photons/keV)	1/e Decay time (ns)	Wavelength of maximum emission (nm)	Refractive index (gm/cm^3)	Density	Z_{eff}	Hygroscopic
$LaBr_3$(Ce)	63	16	380	1.9	5.08	45.22	yes
BaF_2(fast component)	1.8	0.6-0.8	220	1.54	4.88	50.96	slightly
BaF_2(slow component)	10	630	310	1.50	4.88	50.96	slightly
NaI(Tl)	38	250	415	1.85	3.67	50.6	yes
LSO	32	41	420	1.81	7.1	65.5	no
CsI(Tl)	54	1000	550	1.79	4.51		slightly

The data presented here are taken from Saint-Gobain scintillation detector operating manual.

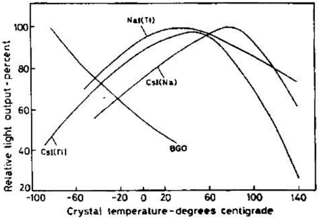

Figure: Response of various inorganic scintillators with temperature

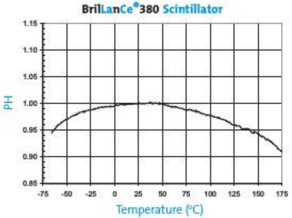

Figure: Response of $LaBr_3$(Ce) scintillator with temperature

Light emission spectra for different inorganic crystals

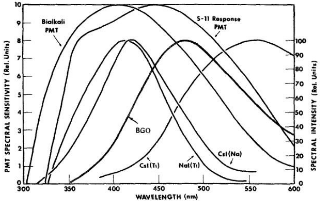

Figure: Emission spectra of several inorganic scintillators

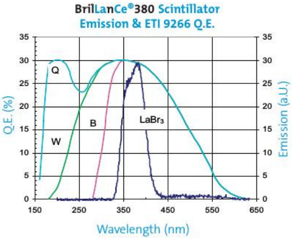

Figure: Scintillation emission spectrum of the BrilLanCe 380 crystal and Quantum Efficiency of a bialkali ETI9266 PMT with (B)Borosilicate, (W)UV glass, and (Q)Quartz face plates

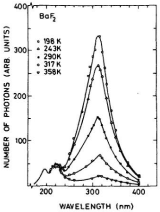

Figure: Scintillation emission spectra from BaF_2 measured at various temperatures

Anode pulse of BaF_2 detector (slow and fast component)

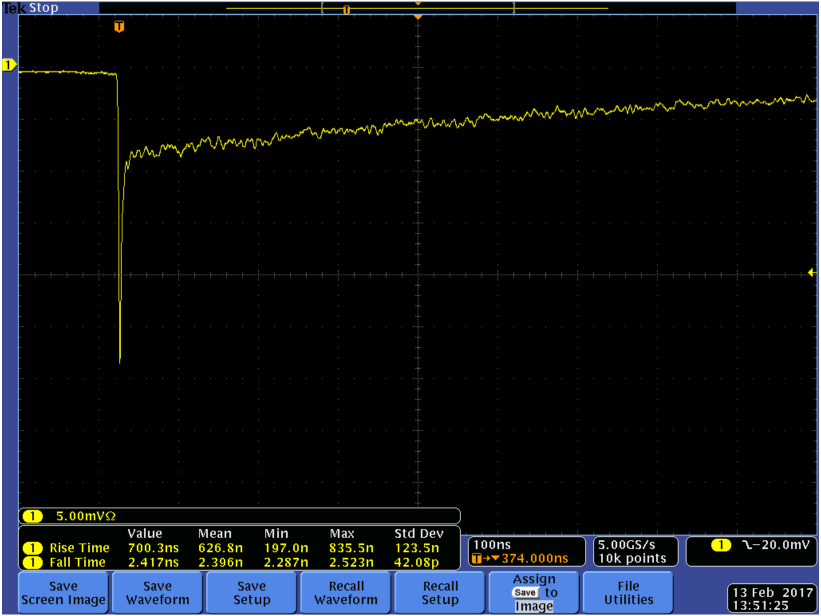

Anode pulse of $LaBr_3(Ce)$ detector

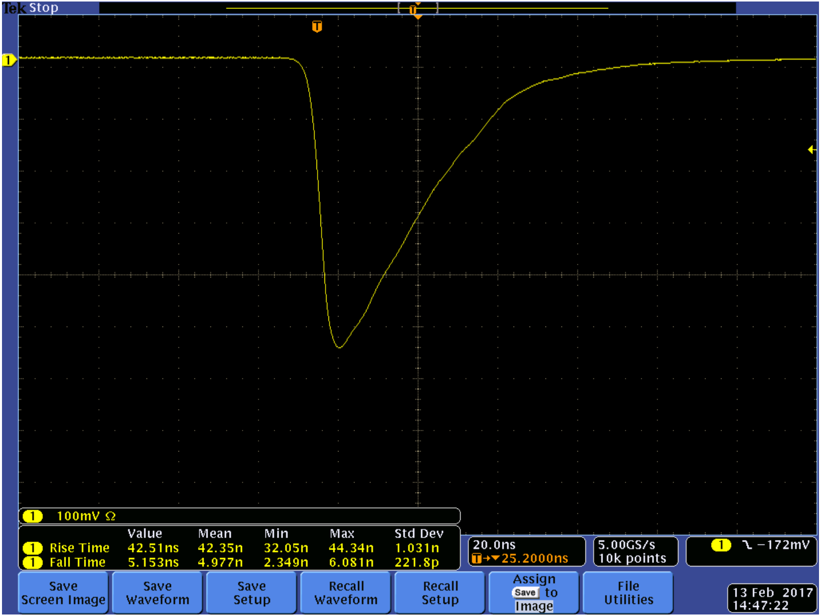

Energy resolutions of $LaBr_3(Ce)$ and BaF_2 scintillation detectors

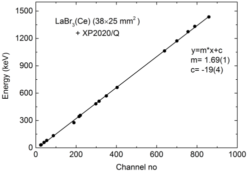

Figure: Energy calibration of $LaBr_3(Ce)$ scintillation detector

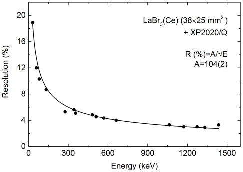

Figure: Energy resolution of $LaBr_3(Ce)$ with γ-ray energy

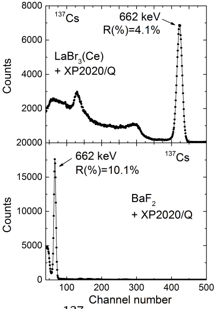

Figure: γ-ray spectra of ^{137}Cs showing relative light output of $LaBr_3(Ce)$ and BaF_2. PMT, HV, amplifier settings remain same.

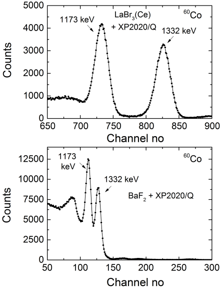

Figure: Difference in energy resolution between $LaBr_3(Ce)$ and BaF_2 scintillators for ^{60}Co γ-ray source

Prompt time resolutions of $LaBr_3(Ce)$ and BaF_2 scintillators

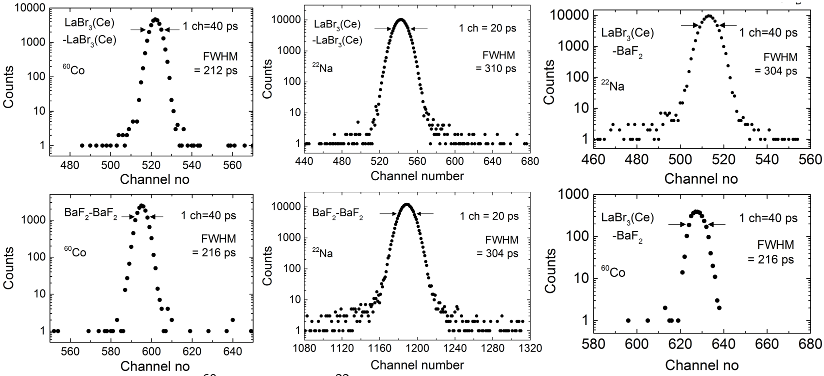

Figure: Prompt time spectra of ^{60}Co (left panel) and ^{22}Na (middle) γ-rays of $LaBr_3(Ce)$-$LaBr_3(Ce)$ detector combination as well as BaF_2-BaF_2 detector combination. Right panel shows prompt time spectra of ^{22}Na and ^{60}Co γ-rays of $LaBr_3(Ce)$-BaF_2 detector combination. Crystal sizes : 38 $\times$ 25 mm^2; PMT : XP2020/Q

Time differential perturbed angular correlation

- The time differential perturbed angular correlation (TDPAC) technique measures the effect of perturbations of the γ-γ angular correlation of the probe nucleus through the hyperfine interaction.
- The nuclear moments (electric quadrupole moment or magnetic dipole moment) of the intermediate level of probe nucleus interact with the hyperfine fields (electric field gradients or magnetic field) present in the investigated sample
- Using this technique, stuctural and magnetic properties of crystalline solids can be studied. Measured electic field gradients by this technique can be compared with the density functional theory (DFT) based calculations.

Time differential perturbed angular correlation

- The time differential perturbed angular correlation (TDPAC) technique measures the effect of perturbations of the γ-γ angular correlation of the probe nucleus through the hyperfine interaction.
- The nuclear moments (electric quadrupole moment or magnetic dipole moment) of the intermediate level of probe nucleus interact with the hyperfine fields (electric field gradients or magnetic field) present in the investigated sample
- Using this technique, stuctural and magnetic properties of crystalline solids can be studied. Measured electic field gradients by this technique can be compared with the density functional theory (DFT) based calculations.

Time differential perturbed angular correlation

- The time differential perturbed angular correlation (TDPAC) technique measures the effect of perturbations of the γ-γ angular correlation of the probe nucleus through the hyperfine interaction.
- The nuclear moments (electric quadrupole moment or magnetic dipole moment) of the intermediate level of probe nucleus interact with the hyperfine fields (electric field gradients or magnetic field) present in the investigated sample
- Using this technique, stuctural and magnetic properties of crystalline solids can be studied. Measured electic field gradients by this technique can be compared with the density functional theory (DFT) based calculations.

Principle of PAC technique

Angular correlation of a γ-γ cascade

$$W(\theta) = \sum_{\substack{k=0 \\ even}}^{k_{max}} A_k P_k(cos\theta), \quad \text{Unperturbed}$$

$$W(\theta, t) = \sum_{\substack{k=0 \\ even}}^{k_{max}} A_k G_k(t) P_k(cos\theta), \quad \text{Perturbed}$$

- A_k : Angular correlation coefficient
- $G_k(t)$: Perturbation function

Nuclear quadrupole interaction

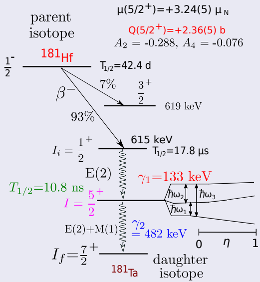

Figure: Decay scheme of the probe ^{181}Hf

Perturbation function

$$G_2(t) = \left[S_{20}(\eta) + \sum_{i=1}^{3} S_{2i}(\eta) cos(\omega_i t) exp(-\delta \omega_i t) \right]$$

- δ: Frequency distribution width arising from lattice imperfections or chemical inhomogeneities
- ω_i: Transition frequencies between the sublevels of the intermediate state which arise due to hyperfine splitting

Schematic diagram of the four detector PAC spectrometer : $LaBr_3(Ce)$-BaF_2 detector setup

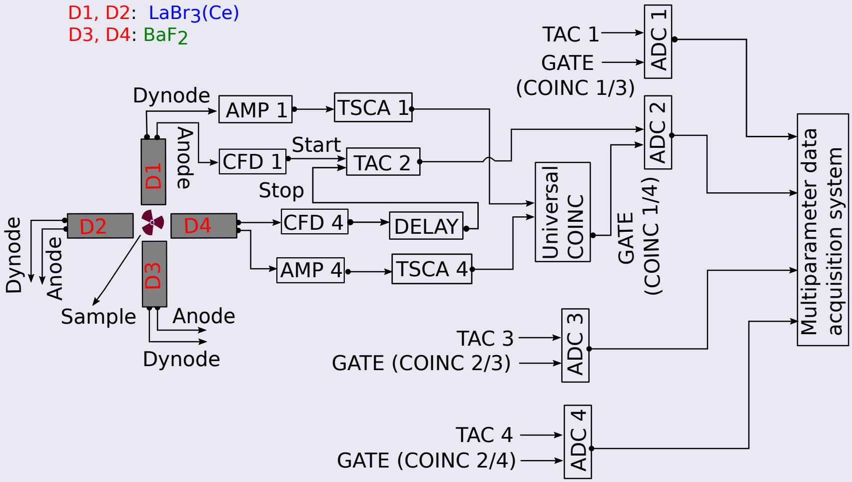

Figure: Slow-fast coincidence set up

Schematic of PAC data reduction

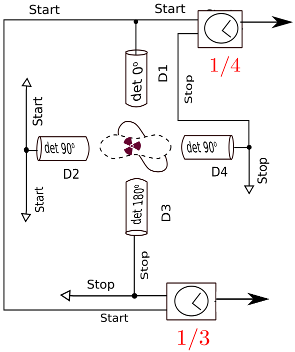

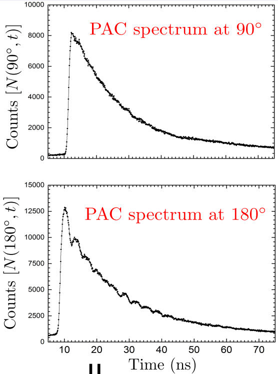

$$W(\theta,t)=1+A_2G_2(t)\mathrm{P}_2(\cos\,\theta)$$

$$N_{ij}(\theta,t) = N_0 exp(-t/\tau_N) W(\theta,t) + B$$

$$R(t) = \frac{2}{3}\left[\sqrt{\frac{N_{13}(180^o,t)N_{24}(180^o,t)}{N_{14}(90^o,t)N_{23}(90^o,t)}} - 1\right]$$

$$A_2G_2(t) = \frac{R(t)}{1+R(t)/2}$$

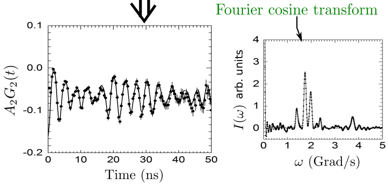

PAC spectrum in stoichiometric sample of $HfNi_3$

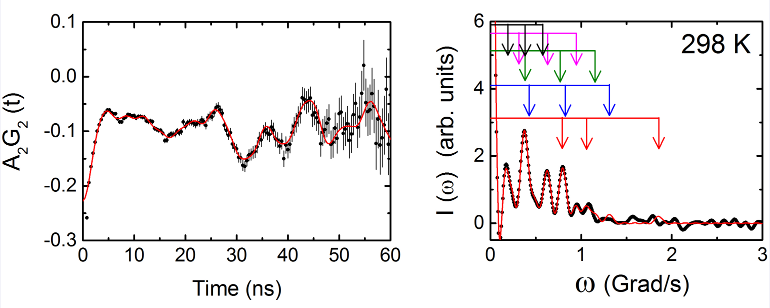

Figure: Figure in the left shows PAC spectrum for the $HfNi_3$ sample at room temperature and the right one shows the corresponding Fourier cosine transform.

Results of PAC measurements in the Hf-Ni sample

Temperature (K)	Component	ω_Q (Mrad/s)	η	δ(%)	f(%)	Assignment
298	1	32.0(3)	0	0	32(2)	$HfNi_3$
	2	52.6(4)	0	0	23(2)	Hf
	3	94.8(6)	0.67(2)	0	14(2)	Hf_8Ni_{21}
	4	70.6(6)	0.38(3)	0	15(2)	$Hf_2Ni_7^{(1)}$
	5	64.3(8)	0	0	16(2)	$Hf_2Ni_7^{(2)}$

1. S. K. Dey, C. C. Dey, S. Saha, J. Belošević-Čavor, Intermetallics 84 (2017) 112.
2. S. K. Dey, C. C. Dey, S. Saha, J. Phys. Chem. Solids 95 (2016) 98.
3. P.R.J. Silva, H. Saitovitch, J.T. Cavalcante, M. Forker, J. Magn. Magn. Mater. 322 (2010) 1841.

Conclusion

- $LaBr_3(Ce)$ is found to be best scintillator for energy and timing spectroscopy experiments.
- Due to the superior energy and time resolutions of $LaBr_3(Ce)$ detector, it has been possible to distinguish weak EFGs corresponding to different phases that present in the stoichiometric sample of $HfNi_3$ by TDPAC spectroscopy.

Conclusion

- $LaBr_3(Ce)$ is found to be best scintillator for energy and timing spectroscopy experiments.
- Due to the superior energy and time resolutions of $LaBr_3(Ce)$ detector, it has been possible to distinguish weak EFGs corresponding to different phases that present in the stoichiometric sample of $HfNi_3$ by TDPAC spectroscopy.

Thank You